

Baryon topology in hypersphere soliton model

Soon-Tae Hong*

Center for Quantum Spacetime and Department of Physics, Sogang University, Seoul 04107, Korea

(Dated: October 29, 2021)

Exploiting a topological soliton on a hypersphere, we construct nucleon charge profile functions and find the density distributions for proton and neutron plotted versus the hypersphere third angle μ . The neutron charge density is shown to possess a nontrivial μ dependence, consisting of both positive and negative charge density fractions. We next investigate the inner topology of the hypersphere soliton, by making use of the schematic Möbius strips which are related with the tubular neighborhood of half-twist circle in the manifold S^3 . In particular, we find that in the hypersphere soliton the nucleons are delineated in terms of a knot structure of two Möbius strip type circles in S^3 . Moreover, the two Hopf-linked Möbius strip type circles in the hypersphere soliton are shown to correspond to (uu, d) in proton and (dd, u) in neutron, respectively, in the quark model.

Keywords: hypersphere soliton, baryon, charge density profiles, knot, twist circle

I. INTRODUCTION

It is well known that the Dirac Hamiltonian scheme has been employed [1–4], to convert the second class constraints into the first class ones. Moreover, making use of the Dirac quantization, there have been many attempts for quantizing the constrained systems, in order to obtain rigorous energy spectrum and investigate BRST [5–7] symmetries involved in the systems. In particular, the first order tetrad gravity has been investigated in the Dirac Hamiltonian scheme to see that the second class constraints reduce the theory to second order tetrad gravity and the first class constraints are different from those in the second order formalism, but satisfy the same gauge algebra if one uses Dirac brackets [2]. There have been attempts to study the quantum BRST charge for quadratically nonlinear Lie algebras, and to derive a condition which is necessary and sufficient for the existence of a nilpotent BRST charge [3]. In a (1+1) dimensional supersymmetric soliton, topological boundary conditions and the BPS bound have also been investigated to fix ambiguities in the quantum mass of the soliton [8]. Moreover the Hamiltonian constraint approach has been applied to the cosmological perturbation theory [9, 10], and to the supersymmetric self-dual loop quantum cosmology [11].

On the other hand, it is well known that the standard Skyrmon model [4, 12–14] is a constrained Hamiltonian system. In particular, the Skyrmon has been analyzed via the canonical quantization in the second class formalism, to study the baryon kinematics and its static properties [13]. Later, the hypersphere soliton model (HSM) has been proposed on the curved manifold [15] to obtain a topological lower bound on the baryon soliton energy and a set of equations of motion. Next we have newly predicted the baryon physical properties, such as masses, charge radii and magnetic moments in the HSM [14].

Recently we have studied a mechanism of baryon mass genesis by exploiting a pulsating soliton in HSM [16]. To do this, first we have exploited the first class Hamiltonian to quantize the hypersphere soliton, and then have predicted the axial coupling constant whose value is comparable to its corresponding experimental data. Next we have formulated the intrinsic frequencies of the pulsating baryons. Explicitly, we have evaluated the intrinsic frequencies ω_N and ω_Δ of the nucleon and delta hyperon, respectively, to obtain the identity $\omega_\Delta = 2\omega_N$.

In this paper we will consider the HSM, to study the baryon phenomenology and profile functions inside baryons. We will also construct nucleon charge profile functions and depict the density distributions for proton and neutron plotted versus the hypersphere third angle μ . As a result, we will find that the neutron charge density has a nontrivial μ dependence. Next, in the HSM, we will investigate the knot structure of the Möbius strips associated with the tubular neighborhood of the half-twist circle inside the topological soliton. Moreover, we will consider two Hopf-linked [17, 18] Möbius strip type circles in the HSM, to show that they correspond to (uu, d) and (dd, u) combinations for the proton and neutron, respectively, in the quark model.

In Sec. II, we will briefly recapitulate baryon formalism to study the profile function inside the baryons. In Sec. III, we will analyze the charge profile functions of nucleons. In Sec. IV, we will investigate the knot structures of the Möbius strip type half-twist circles inside the nucleons. Sec. V includes conclusions. In Appendix A, hypersphere geometry is summarized, and the Hopf fibration [19–21] is discussed on the hypersphere.

*Electronic address: galaxy.mass@gmail.com

II. BARYON CHARACTERISTICS IN HSM

In this section, we exploit the HSM [14–16] to briefly study the baryon phenomenology and the profile function in Fig. 1(a) in the identity map associated with the BPS bound in the baryon soliton energy. To do this, we start with the Skyrme Lagrangian density

$$\mathcal{L} = \frac{f_\pi^2}{4} \text{tr}(\partial_\mu U^\dagger \partial^\mu U) + \frac{1}{32e^2} \text{tr}[U^\dagger \partial_\mu U, U^\dagger \partial_\nu U]^2, \quad (2.1)$$

where U is an $SU(2)$ chiral field, and f_π and e are a pion decay constant and a dimensionless Skyrme parameter, respectively. Next the quartic term is necessary to stabilize the soliton in the baryon sector. Now we proceed to investigate baryon phenomenology by using the three-sphere metric given in Appendix A

$$ds^2 = \lambda^2 d\mu^2 + \lambda^2 \sin^2 \mu (d\theta^2 + \sin^2 \theta d\phi^2). \quad (2.2)$$

Here the ranges of the hyperspherical coordinates are given by $0 \leq \mu \leq \pi$, $0 \leq \theta \leq \pi$ and $0 \leq \phi \leq 2\pi$, and λ ($0 \leq \lambda < \infty$) is the radius parameter of the hypersphere S^3 . Note that S^3 is described in terms of the three dimensional hypersphere coordinates (μ, θ, ϕ) and the radius parameter λ .

In the hypersphere soliton on S^3 , we obtain the soliton energy [14–16]

$$E = \frac{f_\pi}{e} \left[2\pi L \int_0^\pi d\mu \sin^2 \mu \left(\left(\frac{df}{d\mu} + \frac{1}{L} \frac{\sin^2 f}{\sin^2 \mu} \right)^2 + 2 \left(\frac{1}{L} \frac{df}{d\mu} + 1 \right)^2 \frac{\sin^2 f}{\sin^2 \mu} \right) + 6\pi^2 \right], \quad (2.3)$$

where $L = ef_\pi \lambda$ ($0 \leq L < \infty$) is a radius parameter expressed in dimensionless units. Here $f(\mu)$ is the profile function for the hypersphere soliton, and satisfies $f(0) = \pi$ and $f(\pi) = 0$ for unit baryon number. The above soliton energy has the BPS bound in the soliton model [14–16, 21, 22] to yield the inequality

$$E \geq \frac{6\pi^2 f_\pi}{e} |B|, \quad (2.4)$$

where B is given by [14]

$$B = -\frac{2}{\pi} \int_0^\pi d\mu \sin^2 \mu f \frac{df}{d\mu}. \quad (2.5)$$

Note that B is a conserved topological charge which is a baryon number in the HSM. For a single soliton, the topological charge is one [14–16, 21, 22]. In the cases of multi-Skyrmion solutions with $|B| > 1$, the soliton energies will not satisfy the bound in Eq. (2.4) and possess much higher energy. The hedgehog solutions for the multi-Skyrmions then have been shown to be almost certainly all unstable saddle-points of the energy [21].

The profile function f in the soliton energy lower bound satisfies equations of motion [14, 15],

$$\frac{df}{d\mu} + \frac{1}{L} \frac{\sin^2 f}{\sin^2 \mu} = 0, \quad \frac{1}{L} \frac{df}{d\mu} + 1 = 0. \quad (2.6)$$

One of the simplest solutions of (2.6) is the identity map [14–16]

$$f(\mu) = \pi - \mu \quad (2.7)$$

with the condition $L = L_B$, where $L_B \equiv ef_\pi \lambda_B = 1$. The profile function $f(\mu)$ in the identity map, associated with the BPS bound in the soliton energy, is depicted in terms of the angle μ in Fig. 1(a). The fixed value $L = L_B$ can be used to obtain the soliton energy lower bound [14–16]¹

$$E = \frac{6\pi^2 f_\pi}{e}. \quad (2.8)$$

¹ From now on we will use the condition $L_B = 1$ to predict the physical quantities such as moment of inertia, baryon masses and charge radii in the HSM. We will then write the results for the identity map after the integral or definition expressions in (2.10), (2.12) and (3.2).

After performing the Dirac quantization in the first class formalism [1, 4], we obtain the modified Hamiltonian spectrum [4, 16]

$$\langle H \rangle = E + \frac{1}{2\mathcal{I}} \left[I(I+1) + \frac{1}{4} \right], \quad (2.9)$$

where I ($= 1/2, 3/2, \dots$) are isospin quantum numbers of baryons. Here E is given by (2.8) and \mathcal{I} is the moment of inertia [14]

$$\mathcal{I} = \frac{8\pi}{3e^3 f_\pi} \int_0^\pi d\mu \sin^2 \mu \sin^2 f \left(1 + \left(\frac{df}{d\mu} \right)^2 + \frac{\sin^2 f}{\sin^2 \mu} \right) = \frac{3\pi^2}{e^3 f_\pi}. \quad (2.10)$$

As a result, exploiting (2.9) we construct the Weyl ordering corrected nucleon and delta hyperon masses, respectively [16]

$$M_N = ef_\pi \left(\frac{6\pi^2}{e^2} + \frac{e^2}{6\pi^2} \right), \quad M_\Delta = ef_\pi \left(\frac{6\pi^2}{e^2} + \frac{2e^2}{3\pi^2} \right). \quad (2.11)$$

Next, in the HSM we obtain the electric isovector mean square charge radius $\langle r^2 \rangle_{E,I=1}$ of the form [14]

$$\langle r^2 \rangle_{E,I=1} = \frac{8\pi}{3e^2 f_\pi^2 \tilde{\mathcal{I}}} \int_0^\pi d\mu \sin^4 \mu \sin^2 f \left(1 + \left(\frac{df}{d\mu} \right)^2 + \frac{\sin^2 f}{\sin^2 \mu} \right) = \frac{5}{6e^2 f_\pi^2}, \quad (2.12)$$

where $\tilde{\mathcal{I}}$ is the dimensionless moment of inertia defined as $\tilde{\mathcal{I}} = e^3 f_\pi \mathcal{I}$. Similarly, we find the other charge radii in the HSM to yield [14, 16]

$$\langle r^2 \rangle_{E,I=1}^{1/2} = \langle r^2 \rangle_{M,I=0}^{1/2} = \langle r^2 \rangle_{M,I=1}^{1/2} = \langle r^2 \rangle_{M,p}^{1/2} = \langle r^2 \rangle_{M,n}^{1/2} = \sqrt{\frac{5}{6}} \frac{1}{ef_\pi}, \quad (2.13)$$

where the subscripts E and M stand for the electric and magnetic radii, respectively.

Making use of the charge radii in (2.13) we fix the value of $\langle r^2 \rangle_{M,p}^{1/2}$ with the corresponding experimental data $\langle r^2 \rangle_{M,p}^{1/2} = 0.80$ fm. We then have

$$ef_\pi = 225.23 \text{ MeV} = (0.876 \text{ fm})^{-1}. \quad (2.14)$$

Note that, inserting $ef_\pi = (0.876 \text{ fm})^{-1}$ into the condition $L_B = 1$, we obtain $\lambda_B = 0.876$ fm. The hypersphere soliton is thus defined in terms of the fixed radius parameter λ_B which is comparable to the predictions for the charge radii in (2.13). In other words, in the HSM the universe \mathcal{U} is given by a sum of two subspaces, namely $\mathcal{U} = V_B(\lambda \leq \lambda_B) \oplus \bar{V}_B(\lambda > \lambda_B)$ where $V_B(\lambda \leq \lambda_B)$ and $\bar{V}_B(\lambda > \lambda_B)$ are the volume subspaces inside and outside the hypersphere soliton, respectively. Moreover, in HSM the baryons are described in terms of V_B which is a three dimensional volume defined inside S^3 having the volume element in (A.4). Note that most of baryon charges are located inside the volume V_B of radius parameter λ_B as shown in (2.13). Explicitly $\langle r^2 \rangle_{M,p}^{1/2} = \sqrt{\frac{5}{6}} \lambda_B = 0.91 \lambda_B$, for instance.

Finally note also that the hypersphere coordinates (μ, θ, ϕ) are integrated out in (2.3), and E in (2.8) is a function of $\lambda_B = \frac{1}{ef_\pi}$ or equivalently f_π and e only. Moreover, similar to E in (2.3) and B in (2.5), the above physical quantities such as the moment of inertia and charge radii are also given by integral expressions, as in (2.10) and (2.12) for instance. These physical quantities are thus obtained in terms of f_π and e only.

III. CHARGE DENSITY PROFILES IN HSM

In this section, we investigate the charge density profiles of nucleons in Fig. 1(b) and Fig. 1(c). Note that, as in the the profile function in the identity map in Fig. 1(a), these charge density profiles are formulated in terms of the angle μ . Moreover the charge density profiles $\rho_p(\mu)$ and $\rho_n(\mu)$ are associated with the charges inside the nucleons, while the profile function $f(\mu)$ in the identity map is related with the BPS bound in the soliton energy.

Now, using the three-sphere metric in (2.2), we construct the charge density profiles of proton and neutron

$$\rho_p(\mu) = \frac{1}{2} [\rho_{I=0}(\mu) + \rho_{I=1}(\mu)], \quad \rho_n(\mu) = \frac{1}{2} [\rho_{I=0}(\mu) - \rho_{I=1}(\mu)], \quad (3.1)$$

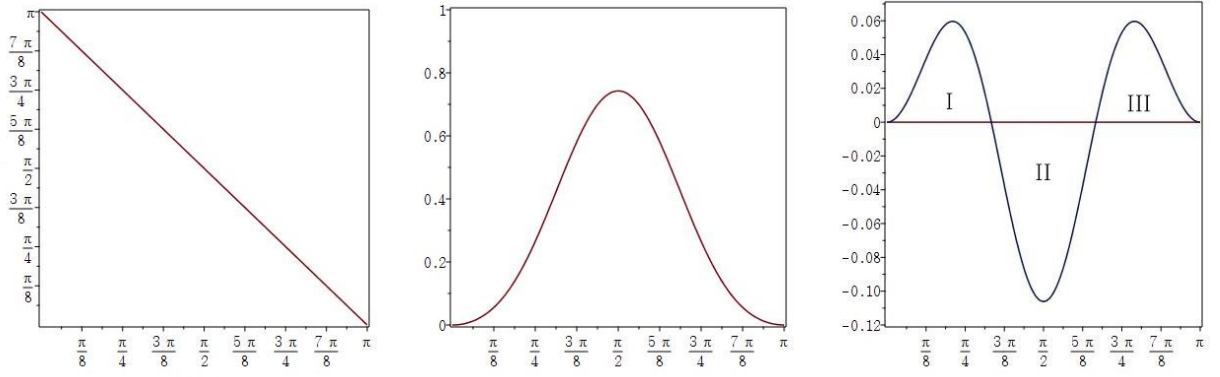


FIG. 1: (a) The profile function $f(\mu)$ in the identity map, and the charge density profiles (b) $\rho_p(\mu)$ and (c) $\rho_n(\mu)$, for proton and neutron respectively, are plotted versus μ . Here $f(\mu)$ is related with the BPS bound in the soliton energy, and $\rho_p(\mu)$ and $\rho_n(\mu)$ are associated with the charges inside the nucleons.

where the isoscalar and isovector electric charge densities are given by [14]

$$\begin{aligned}\rho_{I=0}(\mu) &= -\frac{2}{\pi} \sin^2 f \frac{df}{d\mu} = \frac{2}{\pi} \sin^2 \mu, \\ \rho_{I=1}(\mu) &= \frac{8\pi}{3\tilde{L}} \sin^2 \mu \sin^2 f \left(1 + \left(\frac{df}{d\mu} \right)^2 + \frac{\sin^2 f}{\sin^2 \mu} \right) = \frac{8}{3\pi} \sin^4 \mu,\end{aligned}\quad (3.2)$$

respectively, to produce

$$\rho_p(\mu) = \frac{1}{\pi} \sin^2 \mu \left(1 + \frac{4}{3} \sin^2 \mu \right), \quad \rho_n(\mu) = \frac{1}{\pi} \sin^2 \mu \left(1 - \frac{4}{3} \sin^2 \mu \right). \quad (3.3)$$

We then find the proton and neutron charges as follows

$$Q_p = \int_0^\pi d\mu \rho_p(\mu), \quad Q_n = \int_0^\pi d\mu \rho_n(\mu), \quad (3.4)$$

which yield $Q_p = 1$ and $Q_n = 0$ as expected.

The proton and neutron charge densities in (3.3) are depicted in Fig. 1(b) and Fig. 1(c), respectively. From (3.3) we find two root values of $\rho_n(\mu)=0$: $\mu = \frac{\pi}{3}$ and $\mu = \frac{2\pi}{3}$. We now have three regions I, II and III in the neutron charge density as shown in Fig. 1(c) and for each region, we obtain the charge fractions as follows

$$Q_n^I = \frac{\sqrt{3}}{16\pi}, \quad Q_n^{II} = -\frac{\sqrt{3}}{8\pi}, \quad Q_n^{III} = \frac{\sqrt{3}}{16\pi}, \quad (3.5)$$

which are in good agreement with the result $Q_n = 0$. Note that the charge density profiles of proton and neutron have no dependence on the coordinates θ and ϕ and they have dependence only on the coordinate μ on S^1 .²

IV. TOPOLOGY AND KNOT STRUCTURE IN HSM

Now we investigate the topological aspects and knot structure in the hypersphere soliton. To to this, we first consider the (1+1) dimensional sine-Gordon soliton whose Lagrangian is given in appropriate length and energy units

² Note that for a given fixed value of $\mu = \mu_0$, the three-sphere metric in (A.1) becomes $ds^2 = \lambda^2 \sin^2 \mu_0 (d\theta^2 + \sin^2 \theta d\phi^2)$. This two-sphere metric is given by the coordinates (θ, ϕ) and the fixed two-sphere radius parameter $\lambda \sin \mu_0$. The charge density profiles of the nucleons thus do not depend on (θ, ϕ) , but depend on μ for the fixed value of $\mu = \mu_0$ corresponding to the two-sphere radius parameter $\lambda \sin \mu_0$. Here and in Sec. IV and Appendix A, we use λ instead of λ_B for the radius parameter of hypersphere, for simplicity.

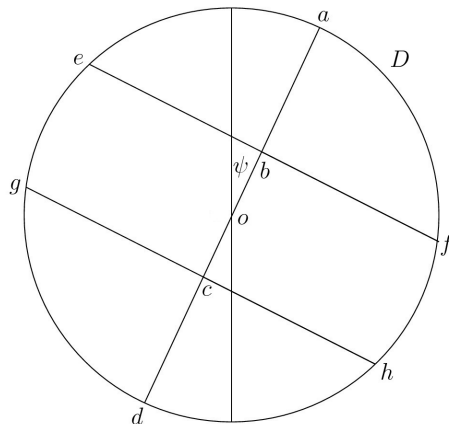


FIG. 2: The cross section of tubular neighborhood of the half-twist circle is delineated by the schematic Möbius strip.

as follows [21, 23–25]

$$L_{SG} = \int dx \left[\frac{1}{2} \partial_\mu \phi \partial^\mu \phi + \cos \phi - 1 \right], \quad (4.1)$$

from which we obtain the field equation of the form

$$\square \phi + \sin \phi = 0. \quad (4.2)$$

Note that the sine-Gordon field equation satisfies the discrete symmetry $\phi(x, t) \rightarrow \phi(x, t) + 2N\pi$, $N = 0, \pm 1, \pm 2, \dots$. The topological charge for a static solution of the sine-Gordon kink is then given by $Q_{top} = \frac{1}{2\pi}[\phi(+\infty) - \phi(-\infty)]$. We now have the static soliton solutions of the form: $\phi(x) = +4 \tan^{-1} \exp x$ and $\phi(x) = -4 \tan^{-1} \exp x$, for the cases of $Q_{top} = +1$ for a kink and $Q_{top} = -1$ for an anti-kink, respectively. These sine-Gordon kink solutions represent infinite Möbius strip feature [24]. Moreover the sine-Gordon kink state is identifiable as a fermion [25]. Note in the hypersphere soliton that, exploiting B in (2.5), we have the profile function $f(\mu) = \pi - \mu$ for the hypersphere soliton with the topological charge $B = +1$ [14, 21]. We also obtain $f(\mu) = -(\pi - \mu)$ for the hypersphere anti-soliton with $B = -1$ [21]. In this sense, in the hypersphere soliton, we have the Möbius strip feature similar to that in the sine-Gordon kink.

Next we consider a *half-twist circle* S^1 inside S^3 which will be discussed in Appendix A, in order to briefly investigate the relations between the three dimensional tubular neighborhood of the half-twist circle and the corresponding Möbius strip. We now assume that the point o is the center of the two dimensional disc D representing the cross section of the tubular neighborhood of the half-twist circle as shown in Fig. 2. Here the line segment ad represents the cross section of the Möbius strip. Next we cut the disc D of the tubular neighborhood into three pieces by using the line segments ef and gh , and then we let the points b and c denote the corresponding cross sectional cutting lines on the Möbius strip. Here ψ represents the rotation angle of the disc D (or the line segment ad) with respect to the vertical line which is the initial position of D . As the disc D rotates along the circle S^1 of radius parameter λ , the angle ψ increases from 0 to π , to complete the cycle of the half-twist. In other words, after the complete rotation the final disc D arrives at the initial disc position, with the angle shift π . By gluing these two discs together, we obtain a Möbius strip type tubular neighborhood of the half-twist circle S^1 . In particular, the tubular neighborhood is splitted into three pieces with nontrivial volume shapes along the half-twist circle. Moreover the line segment ad inside the tubular neighborhood makes the Möbius strip. In this respect without loss of generality, instead of exploiting the tubular neighborhood of the half-twist circle S^1 inside S^3 , for visual clarity we will use the schematic Möbius strips in Fig. 3(a) and Fig. 3(b) in the further discussions for the topology and knot structure of the baryons below. We reemphasize that, in Fig. 3(a) and Fig. 3(b), the Möbius strips represent schematically the tubular neighborhoods of the half-twist circles.

Note that, to describe a fermion such as a nucleon, we need a Möbius strip with a half-twist, associated with a half-twist circle S^1 inside $S^3 (= S^2 \times S^1)$, as shown in Fig. 3(a). For more details about the Möbius strip related with the fermion, see the last paragraph in this section. Here the half-twist circle S^1 plays a major role in the topological structure of the fermion. To relate the HSM to the quark model where, in the fermions such as proton and neutron, there exist three quarks, we separate the Möbius strip into three pieces as shown in Fig. 3(a) to yield two nontrivial



FIG. 3: (a) The schematic Möbius strip in the HSM corresponds to the fermion, and (b) the splitted Möbius strip explains the knot structure of the two different Möbius strip type circles in the hypersphere soliton.

Möbius strips which are Hopf-linked [17, 18] to each other, as shown in Fig. 3(b). More specifically, we have the Möbius strip with the circumference length equal to that of the original Möbius strip in Fig. 3(a) and with a half-twist. This small Möbius strip originates from the middle piece of the Möbius strip in Fig. 3(a). Next we have the other Möbius strip with the circumference length of two times that of the original Möbius strip in Fig. 3(a) and with two twists. This large Möbius strip consists of the first and third pieces of the Möbius strip in Fig. 3(a). Note that the two twists of the large Möbius strip are equal to two times addition of two half-twists of the first and third pieces of the original Möbius strip. Moreover the large strip corresponds to uu in uud and dd in udd for proton and neutron defined in the quark model, respectively. Now we emphasize that two Möbius strips in Fig. 3(b) are Hopf-linked to produce a knot structure, which will be also discussed in Appendix A.

Now we return to exploiting the tubular neighborhood of the half-twist circle in the HSM defined on the hypersphere S^3 , instead of using the schematic Möbius strip. As a result, we find that there exists inside the nucleon the half-twist circle $S^1(\subset S^3)$ possessing the Möbius strip type tubular neighborhood as shown in Fig. 3(a). The tubular neighborhood is now splitted into three pieces along the half-twist circle to yield two Hopf-linked sub-manifolds due to the Möbius strip characteristic of the tubular neighborhood as shown in Fig. 3(b). Indeed, the two Hopf-linked Möbius strip type circles in Fig. 3(b) explains the knot structure of the two different Möbius strip type circles, which correspond to (uu, d) in proton and (dd, u) in neutron, respectively, in the quark model. For more details about the two Hopf-linked circles inside S^3 , see Appendix A.

Finally we classify the boson and fermion in terms of the strip structures. The boson performs 2π rotation to return its starting situation. The feature is explained by exploiting 2π rotation on the ordinary strip. Next the fermion performs 4π rotation to return its initial situation according to the relativistic quantum mechanics. The characteristic is elucidated by using 4π rotation on the Möbius strip shown in Fig. 3(a). The baryonic inner structure is thus successfully explained on the hypersphere S^3 . In contrast, in the case of bosonic inner structure, we do not need to consider such a hypersphere geometry.

V. CONCLUSIONS

In summary, in the HSM we have performed the first class Dirac quantization, to predict more rigorously the physical quantities such as the baryon masses and charge radii. To do this, we have exploited the identity map associated with the BPS bound in the baryon soliton energy. Moreover we have investigated the charge density profile functions of nucleons, and then depicted the density distributions for proton and neutron plotted versus the hypersphere third angle μ . In particular, the neutron charge density has been shown to have the nontrivial μ dependence, consisting of both the positive and negative charge density parts. Next we have investigated the inner topological structures of the hypersphere soliton, by using the Möbius strip type tubular neighborhood of the half-twist circle in S^3 . In particular, we have shown that, in the HSM, the nucleons are described by the knot of two Hopf-linked Möbius strip type circles inside the nucleons. As a result, we have found that the two Hopf-linked Möbius strip type circles in the HSM correspond to the (uu, d) in proton and (dd, u) in neutron, respectively, in the quark model.

Acknowledgments

The author would like to thank Professor Peter van Nieuwenhuizen for helpful correspondence and kind encouragement. He was supported by Basic Science Research Program through the National Research Foundation of Korea

funded by the Ministry of Education, NRF-2019R1I1A1A01058449.

Appendix A: Hypersphere geometry

In order to investigate a hypersphere of radius parameter λ , we consider the three-sphere metric on S^3

$$ds^2 = \lambda^2 d\mu^2 + \lambda^2 \sin^2 \mu (d\theta^2 + \sin^2 \theta d\phi^2). \quad (\text{A.1})$$

The ranges of the hyperspherical coordinates are given by $0 \leq \mu \leq \pi$, $0 \leq \theta \leq \pi$ and $0 \leq \phi \leq 2\pi$, and λ ($0 \leq \lambda < \infty$) is the radius parameter of S^3 . On the hypersphere, the three-sphere metric is given by the line element

$$d\vec{l} = \hat{e}_\mu \lambda d\mu + \hat{e}_\theta \lambda \sin \mu d\theta + \hat{e}_\phi \lambda \sin \mu \sin \theta d\phi, \quad (\text{A.2})$$

where $(\hat{e}_\mu, \hat{e}_\theta, \hat{e}_\phi)$ are the unit vectors along the three directions.

The area elements are given by

$$d\vec{a}_\mu = \hat{e}_\mu \lambda^2 \sin^2 \mu \sin \theta d\theta d\phi, \quad d\vec{a}_\theta = \hat{e}_\theta \lambda^2 \sin \mu \sin \theta d\mu d\phi, \quad d\vec{a}_\phi = \hat{e}_\phi \lambda^2 \sin \mu d\mu d\theta, \quad (\text{A.3})$$

and the three dimensional volume element is defined as

$$dV = \lambda^3 \sin^2 \mu \sin \theta d\mu d\theta d\phi. \quad (\text{A.4})$$

In the hyperspherical coordinates system, the gradient operator is given by

$$\nabla = \hat{e}_\mu \frac{1}{\lambda} \frac{\partial}{\partial \mu} + \hat{e}_\theta \frac{1}{\lambda \sin \mu} \frac{\partial}{\partial \theta} + \hat{e}_\phi \frac{1}{\lambda \sin \mu \sin \theta} \frac{\partial}{\partial \phi}. \quad (\text{A.5})$$

Next, we investigate a half-twist circle $S^1(\subset S^3)$ on the hypersphere. For the space manifolds S^3 and S^2 , we have the homotopy group [21, 26, 27] $\Pi_3(S^2) = \mathbf{Z}$. Note that in the homotopy group, the target space S^2 is a geometrical manifold. Due to the above homotopy group, we have an associated integer topological charge, namely the Hopf charge [21]. Here the Hopf charge is intrinsically different from the topological charge B associated with $\Pi_3(S^3) = \mathbf{Z}$. In other words, one cannot construct any Hopf charge having a form similar to B in (2.5). Instead, we have the preimage of a point on the target manifold S^2 which is a closed loop inside S^3 [21]. Moreover it is shown in the Hopf fibration [19–21] that the closed loop is a half-twist circle $S^1(\subset S^3)$. To be specific, noting that the homology groups for S^3 and $S^2 \times S^1$ are given by $H_1(S^3) = 0$ and $H_1(S^2 \times S^1) = \mathbf{Z}$ [28], one finds that the hypersphere S^3 is *locally* a product of two manifolds $S^3 = S^2 \times S^1$ [29], implying that the $S^1(\subset S^3)$ is the *half-twist* circle of radius parameter λ . It is also interesting to note that the preimages inside S^3 decompose the hypersphere into a continuous family of circles, and two distinct circles are linked inside S^3 [20, 21] and form the Hopf link [17, 18].

-
- [1] P.A.M. Dirac, *Lectures on Quantum Mechanics* (Yeshiva University Press, New York, 1964).
 - [2] L. Castellani, P. van Nieuwenhuizen, M. Pilati, *First order tetrad gravity in Dirac's Hamiltonian formalism*, Phys. Rev. D **26**, 352 (1982).
 - [3] K. Schoutens, A. Sevrin, P. van Nieuwenhuizen, *Quantum BRST charge for quadratically nonlinear Lie algebras*, Commun. Math. Phys. **124**, 87 (1989).
 - [4] S.T. Hong, *BRST Symmetry and de Rham Cohomology* (Springer, Heidelberg, 2015), and references therein.
 - [5] C. Becchi, A. Rouet, R. Stora, *The Abelian Higgs-Kibble model. unitarity of the S operator*, Phys. Lett. B **52**, 344 (1974).
 - [6] C. Becchi, A. Rouet and R. Stora, *Renormalization of gauge theories*, Ann. Phys. **98**, 287 (1976).
 - [7] I.V. Tyutin, *Gauge invariance in field theory and statistical physics in operator formalism*, Lebedev preprint, LEBEDEV-75-39 (1975), arXiv:0812.0580.
 - [8] H. Nastase, M. Stephanov, P. van Nieuwenhuizen and A. Rebhan, *Topological boundary conditions, the BPS bound, and elimination of ambiguities in the quantum mass of solitons*, Nucl. Phys. B **542**, 471 (1999), hep-th/9802074.
 - [9] D. Langlois, *Hamiltonian formalism and gauge invariance for linear perturbations in inflation*, Class. Quantum Grav. **11**, 389 (1994).
 - [10] P. Mankiewicz, *Hamiltonian formalism and gauge-fixing conditions for cosmological perturbation theory*, Class. Quantum Grav. **36**, 215003 (2019), arXiv:1810.11621.
 - [11] K. Eder and H. Sahlmann, *Supersymmetric minisuperspace models in self-dual loop quantum cosmology*, JHEP **03**, 064 (2021), arXiv:2010.15629.
 - [12] T.H.R. Skyrme, *A nonlinear field theory*, Proc. R. Soc. Lond. A **260**, 127 (1961).

- [13] G.S. Adkins, C.R. Nappi, E. Witten, *Static properties of nucleons in the Skyrme model*, Nucl. Phys. B **228**, 552 (1983).
- [14] S.T. Hong, *The static properties of Skyrmions on a hypersphere*, Phys. Lett. B **417**, 211 (1998) [Corrigendum-ibid. **803**, 135179 (2020)].
- [15] N.S. Manton, P.J. Ruback, *Skyrmions in flat space and curved space*, Phys. Lett. B **181**, 137 (1986).
- [16] S.T. Hong, *Dirac quantization and baryon mass genesis in hypersphere soliton model*, arXiv:2105.11456.
- [17] L.H. Kauffman, *On Knots* (Princeton University Press, Princeton, 1987).
- [18] J. Baez, J.P. Muniain, *Gauge Fields, Knots and Gravity* (World Scientific, Singapore, 1994).
- [19] H. Hopf, *Über die abbildungen der dreidimensionalen sphäre auf die kugelfläche*, Math. Ann. **104**, 637 (1931).
- [20] R. Bott, L.W. Tu, *Differential Forms in Algebraic Topology* (Springer, New York, 1982).
- [21] N.S. Manton, P. Sutcliffe, *Topological Solitons* (Cambridge University Press, Cambridge, 2004).
- [22] L.D. Faddeev, *Some comments on the many-dimensional solitons*, Lett. Math. Phys. **1**, 289 (1976).
- [23] T.H.R. Skyrme, *Particle states of a quantized meson field*, Proc. R. Soc. Lond. A **262**, 237 (1961).
- [24] L.J. Boya, J. Mateos, *Group Theoretical Methods in Physics* (Springer-Verlag, Berlin, 1980), Editor: K.B. Wolf.
- [25] R. Rajaraman, *Solitons and Instantons* (North-Holland, Amsterdam, 1987).
- [26] H. Toda, *Composition Methods in Homotopy Groups of Spheres* (Princeton University Press, Princeton, 1962).
- [27] A.S. Schwarz, *Quantum Field Theory and Topology* (Springer-Verlag, Berlin, 1993).
- [28] J.J. Rotman, *An Introduction to Algebraic Topology* (Springer-Verlag, Heidelberg, 1988).
- [29] L.H. Ryder, *Dirac monopoles and the Hopf map $S^3 \rightarrow S^2$* , J. Phys. A: Math. Gen. **13**, 437 (1980).